Submitted: 01/15/20

Research Article

[1]Department of Math, McGill University, Montreal, QC, Canada
[2]Department of Physiology, McGill University, Montreal, QC, Canada

Keywords

Cellular automaton, FitzHugh-Nagumo model, excitable media, cardiac dynamics, convolutional neural network

Email Correspondence

yujing.zou@mail.mcgill.ca

Yujing Zou[1,2], Gil Bub[2]

Comparison of Complexity and Predictability of a Cellular Automaton Model in Excitable Media Cardiac Wave Propagation Compared with a FitzHugh-Nagumo Model

Abstract

Background: Excitable media are spatially distributed systems that propagate signals without damping. Examples include fire propagating through a forest, the Belousov-Zhabotinsky reaction, and cardiac tissue. (1) Excitable media generate waves which synchronize cardiac muscle contraction with each heartbeat. Spatiotemporal patterns formed by excitation waves distinguish healthy heart tissues from diseased ones. (3) Discrete Greenberg-Hastings Cellular- Automaton (CA) (1) and the continuous FitzHugh- Nagumo (FHN) model (7 are two methods used to simulate cardiac wave propagation. However, previous observations have shown that these models are not accurately predictive of experimental results as a function of time. We hypothesize that cardiac simulations deviate from the experimental data at a rate that depends on the complexity of the experimental data's initial conditions (I.C.).

Methods: To test this hypothesis, we investigated two types of propagating waves with different complexities: a planar (i.e. simple) and a spiral wave (i.e. complex). With the same I.C., we first compared simulation results of a Greenberg-Hastings Cellular Automaton (GH-CA) model to that a FitzHugh-Nagumo (FHN) continuous model which we used as a surrogate for experimental data. We then used median-filtered real-time cardiac tissue experimental data to initialize the GH-CA model and observe the divergence of wave propagation in the simulation and the experiment.

Results and Conclusion: The alignment between the CA model of a planar wave and the FHN model remains constant, while the degree of overlap between the CA and FHN models decreases for a spiral wave as a function of time. CA simulation initialized by a planar wave real-time cardiac tissue data propagates like the experimental data, however, this is not the case for the spiral wave experimental data. We were able to confirm our hypothesis that the divergence between the two models are due to initial condition (I.C.) complexity.

Discussion: We discuss a promising strategy to represent a GH-CA model as a Convolutional Neural Network (CNN) to enhance predictability of the model when an initial condition is given by the experimental data with higher level of complexity.

Introduction

An excitable media system can be viewed as a group of coupled individual elements where each element can pass information to its neighbors with various neighborhood size. A signal over a certain threshold initiates a wave of activity moving across the excitable medium. (2) They are spatially distributed systems that propagate signals without damping. An excitable media is characterized by its threshold of excitability, which is a certain level of excitation to be reached before the system can generate travelling waves whose shape and speed remain unchanged through the medium. Examples of travelling waves in excitable media include fire propagating through a forest, the Belousov-Zhabotinsky (BZ) reaction, and propagating waves for means of communication within and across nerves as well as generating contraction (8) in cardiac tissue. (1) More specifically, the heart supports propagating waves in a variety of different geometrical patterns including plane waves, spirals, and multiple spirals. As a physical system passing signals by diffusion, this travelling wave is a result of propagating electrical activity in cardiac muscle involving sodium and potassium ions moving to neighboring cells. (2)

The wave dynamics and the resultant spatiotemporal patterns are essential to the heart's function. (3) Changes in the spatial patterns of these waves can cause potentially deadly arrhythmias, therefore, spatiotemporal patterns formed by excitation waves can distinguish healthy heart tissues from diseased ones. In the context of this paper, we define planar waves as travelling waves emanating from a central pacemaking source that acts to synchronize contraction during a healthy heartbeat. In contrast, aberrant re-entrant waves, which have a characteristic spiral geometry, re-excite the tissue rapidly and underlie potentially deadly tachycardias and fibrillation. (3) We define them as spiral waves. Therefore, a planar wave's initial condition is deemed to have less complexity than that of a spiral wave. We use cardiac monolayers which are thin sheets of heart muscle tissue grown in a petri dish to examine the dynamics of these propagating waves. These cultured cardiac cells can form connections and generate excitation waves which propagate out from an initiating point (a target) or a re-entrant circuit (a circuit of electricity where an impulse re-enters and a region of the heart is repetitively excited) with a spiral shape. Thus, studying these waves from the cardiac monolayers can help improve our understanding of cardiac arrhythmias. (2)

In this paper, we focus on computational methods to study these excitable waves. *Discrete cellular-automaton (CA)* and *continuous FitzHugh-Nagumo (FHN) models* are both well-known systems for simulating cardiac wave propagation. In a cellular automaton model, each cell has a finite number of states. These states are updated based on the states of their neighbors and their own previous state. It is an extremely powerful method for studying the dynamics of an excitable media due to its simple rules which underpin the nature of connected cells, even while the processes driving the physical system can be rather complicated (Fig. 1, first row). However, previous results have demonstrated that neither of the CA and FHN models show consistently accurate predictions of excited wave behaviors that align with experimental results (Fig. 2, second row) after a

few seconds. Consequently, it is crucial to determine the roots of the discrepancies seen between the CA model and experimental result in order to generate an accurate model of the dynamics. Therefore, we hypothesized that cardiac simulations deviate from the experimental data as a function of the complexity of initial conditions (I.C.) of the experimental data.

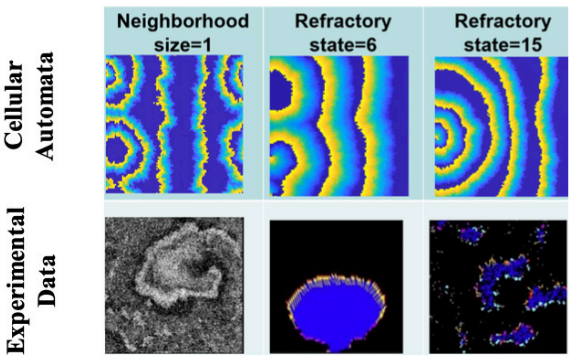

Figure 1. Greenberg-Hastings Cellular Automaton (GH-CA) wave (first row) propagation simulations generated at various parameter values can accurately represent experimental data. The GH-CA algorithm is detailed in section 2.1. The first row shows Cellular Automaton simulations of wave propagation: where the first subfigure shows a planar wave and the second and the third subfigure show a spiral wave with various refractory states where the spiral source is to the very left of the panel. In the second row: the first subfigure is a snapshot of a spiral wave during tachycardia, the second and the third pictures show an example output of wave segmentation and tracking using an automated wave tracking software in cultured cardiac monolayers called 'Ccoffinn'. (4)

The cardiac membrane potential function of the FHN model is continuous. It is relatively simple and not computationally expensive so it was used to produce surrogate data as our "ground truth" for wave propagations. Here, we provide a direct comparison between Greenberg-Hastings Cellular Automaton and FHN model simulations for two types of excited waves with differential complexity, a planar wave I.C. for the simple type and a spiral wave I.C. for the complex type. Our results were able to confirm our hypothesis that when the same I.C. was given, the two models diverge earlier in simulation time steps when the I.C. is more complex.

Methods

To study what gives rise to the divergence between a cellular automaton model and experimental results over time, we investigated two types of propagating waves with different complexity: a planar and a spiral wave. We first built a discrete GH-CA model of size 100 by 100 cells. Then we used diffusively coupled FHN equations to generate surrogate data sets as our "ground truth experimental data" since its (fast and slow) variables together reflect the cardiac membrane potential, which is continuous. We then compared the CA and FHN models with the same initial condition using algorithms to quantify wave behavior.

Greenberg-Hastings Cellular Automaton Model

The GH-CA model follows a simple set of rules to represent the complex physiological processes that result in electrical impulse generation, conduction, and propagation. It does so by representing electrical activity propagation by cardiac action potentials on a discrete lattice of points in space (i.e. representing the volume of the myocardium) as a form of information transmission. The cellular automaton model is made up of discrete integer numbers where each number represents its own state. States in a CA model are categorized as being at rest, excited, or refractory. Important parameters used in the CA rules for governing wave propagation are the following: the threshold (T) where $0<T<1$, the excitatory state (E), the refractory state (R), the resting state (defined as 0), size of the cardiac tissue (N) which is the number of cells in a row of a 2D CA square array, and the neighborhood size (r) which determines the number of neighboring cells that affect the current cell state in next time step. We define a 'cell' state as a discrete integer that represents the state of the cell at position (i,j) in the 2D square matrix. For the wave to progress, the state of each cell must be updated during each generation based on the simple rules we define in our GH-CA model. Let $u_j(t)$ be a cell state at a certain time step (or generation). If $1 \leq u_j(t) \leq E+R$, then $u_j(t+1) = u_j(t) + 1$. In simulations using a neighborhood with square boundaries (a Moore neighborhood), we saw unrealistic sharp edges (Fig.2) in our CA simulations. This is due to the condition for a resting cell (state=0) to become the first state of an excited cell (state=1). For square boundaries, when

$$\frac{\#\ of\ excited\ neighboring\ cells}{total\ \#\ of\ neighboring\ cells} > threshold \text{ (Eq. 1)},$$

a resting state becomes 1. We therefore adapted a method where we created a new coordinate system initially developed by Bub *et al.* (1) into our GH-CA model. This algorithm made the edges of our waves significantly smoother (Fig. 2). Specifically, we re-defined the original coordinate of any cell from (x_0, y_0), where x_0 and y_0 are integer numbers, to $(x_0 + \varepsilon x, y_0 + \varepsilon y)$, where εx and εy are uniformly distributed decimal values between -0.5 and 0.5. We also assigned a random weight S_j to each cell in a 2D GH-CA matrix where S_j is uniformly distributed between 0.5 and 1.5. Here, new coordinates and random weights are assigned to each cell every new time step. Then we compute the distance between a resting cell to all its Moore neighboring cells $D[j,i]$. A resting cell becomes excited if

$$\frac{\sum D[j,i]<r; 0<u_j(t)\leq E,\ S_j}{\sum D[j,i]<r; u_j(t)=0, or\ u_j(t)>E, S_j} > threshold \text{ (Eq. 2) [1]}.$$

This randomization process of the new coordinate system successfully eliminated unwanted edges in our GH-CA simulation with the Moore neighborhood counting method is used (Fig. 2).

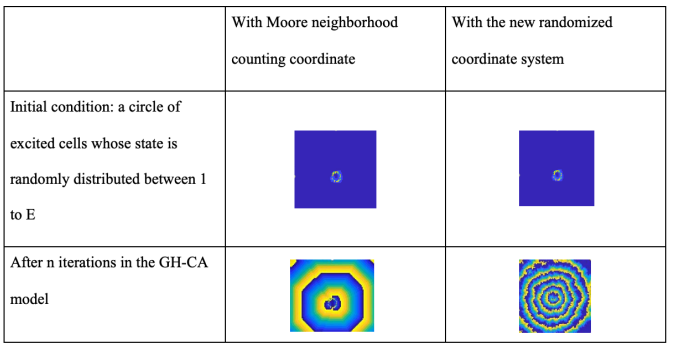

Figure 2. The effect of integrating the new coordinate system into our GH-CA model. We could see in the left column; edge wave front appears in the CA simulation whereas the wavefronts become much smoother when our new coordinate algorithm is adopted.

FitzHugh-Nagumo Equations Model

The FHN model (5) is popular for simulating excitable media because of its analytical tractability (7), relative simplicity, and ease of geometrical analysis. The basic form of the FHN model has two coupled, non-linear ordinary differential equations. One of these depicts the fast evolution of the neuronal membrane voltage while the other equation represents the slower recovery (refractory) action of sodium channel de-inactivation and potassium channel deactivation. For simulating a travelling wave, a spatial diffusion term (i.e. a second derivative in spatial coordinates) is needed for the first equation to model an action potential propagation process, which turns the FHN model into a coupled-diffusive partial differential equation. (7) The electrical propagation properties in an excitable media like nerve fibers are analogous to that of myocardium. Since the model tracks

the membrane voltage continuously and is easily controllable compared to real-time experimental cardiac tissue data, we chose to use the FHN model to create our surrogate cardiac tissue wave propagation dataset as our 'ground truth' to be compared with our GH-CA simulation.

$$\frac{\partial v}{\partial t} = f(v) - r + \frac{D\partial^2 v}{\partial x^2}$$

Where we used $f(v)=-v(a-v)(1-v)$

$$\frac{\partial r}{\partial t} = bv - gr \ \textbf{(Eq. 3)} \ (7)$$

Where we used a=0.25, b=0.001, g=0.003, and D=0.05. The function $f(v)$ is a third order polynomial that describes the fast evolution of the cardiac membrane voltage, whereas the slower recovery variable r provides negative feedback. We used the ode45 solver from Matlab 2018b to solve the above equations (Fig. 3).

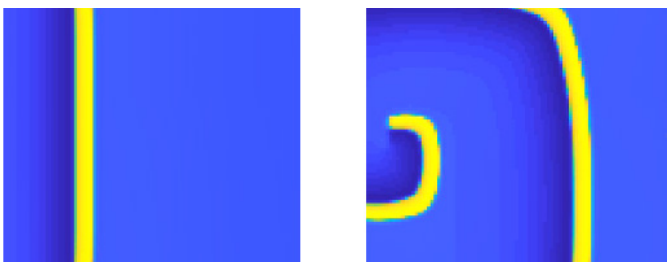

Figure 3. Simulation results of FHN model of a planar wave (left) and a spiral wave (right)

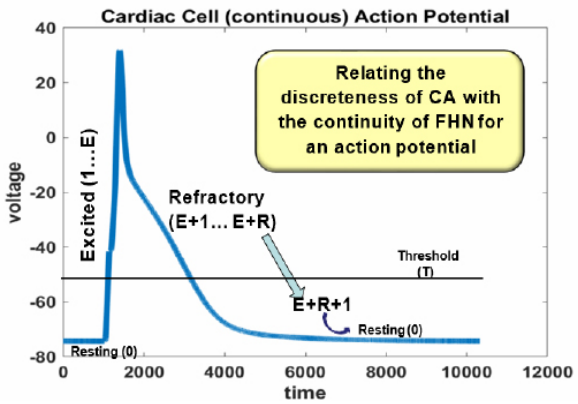

Figure 4. relating the discrete states and parameters of the GH-CA model (i.e. E, R, resting, and T) to an action potential simulated by the FHN model. The GH-CA model simulates cardiac wave propagation whose underlying process is an action potential in discrete states, while the FHN model does so with continuous membrane voltage values. This figure was generated by the Simulink toolbox of Matlab 2018b to simulate a cardiac cell action potential.

Fraction Method

To compare our GH-CA simulation with our FHN surrogate data, we define a measure called the Fraction Method which we used as a first pass to test our hypothesis that GH-CA simulation deviates from our surrogate FHN data at a rate depending on the initial condition complexity. The same initial condition representing a simple (planar) and a complex (spiral) wave were given to both the CA-GH and the FHN model. We computed a ratio of $\frac{\#ofexcitedcells}{\#ofunexcitedcells}$ (Eq. 4) for each iteration of the CA and FHN simulations for both the planar and spiral waves. This algorithm can track wave propagation dynamics regardless of wave travelling direction. A limitation of the Fraction Method has to do with the observation that it does not track the direction of the wave. In other words, the result of the same wave travelling from the left and the right of the 2D CA matrix is the same. However, this method still provides a general sense of wave dynamics regardless of the travelling direction of the wave.

To give the same IC to both models, we initially created a spiral wave from the FHN model. At a certain iteration step of interest in the FHN simulation, we first identified which CA-equivalent state this cell is in, and then directly converted the FHN values into discrete values that corresponded to the state values in a CA model based on the parameter value of a from the FHN model. Let the FHN value be γ. If $0 \leq \gamma < a$, then this cell received an equivalent resting state of 0. If $\gamma > a$ and $\gamma < 1$, then we assumed this cell to be at an excited state; since we would not be sure which discrete state the cell is in, we gave the all FHN values belonging to this range a value of 1 as its excitatory CA state. The rest of the values from the FHN model is assumed to be in a refractory state; similarly, as we do not know the specific state the cell is in, we gave all cells in this FHN value range a state of E+1, the first possible refractory state. This was the initial condition retrieved from our FHN simulation converted into discrete values that our GH-CA model could accept (Fig. 5).

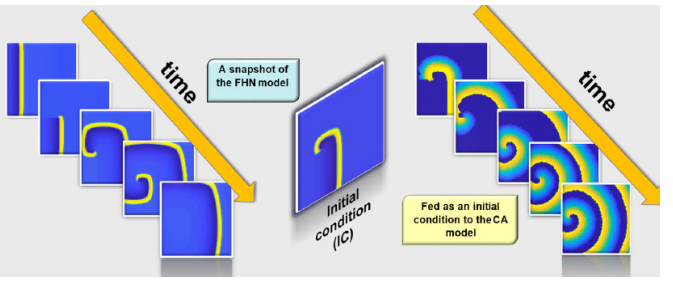

Figure 5. FHN simulation spiral wave propagation (left) where 2D values at a certain instance (middle) were retrieved as an I.C. for the CA, which were then converted into discrete values a GH-CA model can accept (right). This 2D discrete IC was then fed into the GH-CA model which then was let run and created a spiral wave propagation in the GH-CA simulation (right).

Overlap Method

Due to the difference in travelling wave velocity between both models given the same initial condition, the CA simulation always travels seemingly faster than that of the FHN model. Therefore, though the Fraction Method portrays the dynamics for both models, it cannot track how much two simulation with the same initial condition align as a function of time. We then quantify how much the two models overlap in order to test whether differences in initial conditions lead to discrepancies between the GH-CA model and experimental data. Thus, to directly compare the two models, we designed a technique to quantify the degree of overlap between the CA simulation and our 'surrogate' FHN data when both models were given the same initial condition (I.C.) by calculating a ratio of $\frac{\#ofoverlappingcells}{\#ofnon-overlappingcells}$ (Eq. 5) at each time step. We call this ratio the given I.C.'s complexity score. An "overlapping cell" is defined as when a cell is at the same state in both models (i.e. excited, refractory or at rest). This algorithm generates either a spiral or a planar wave in the FHN model, then initializes the GH-CA model with the same initial condition. Due to FHN model's slower wave propagation velocity, we let it iterate 200 steps before starting the GH-CA simulation. We then found the time point of maximal overlap between the two models by determining the ratio in Eq.5 while excluding resting cells with a state of 0. We then iterated the FHN model for another 200 steps and waited for the GH-CA model to achieve the largest match between the two models, then compute the ratio. The same process was repeated for 4 times at five different threshold values of the GH-CA model (Fig. 8).

Using Experimental data as an Initial Condition for the Cellular Automaton Model

We first obtain experimental real-time cardiac activity data (i.e. movies capturing cell's activity frame by frame) that depict a planar wave and a spiral wave from our microscope built by Bub *et al.* published in their *Nature Photonics* paper. (3) With an algorithm written in Python, we con-

verted the experimental data into readable 128 x 128 sized matrix whose further manipulation was performed in Matlab. We then removed the noise from a chosen arbitrary frame using a median filter. After this filtering, this frame's pixel values become integers. For the planar wave (Fig. 5), this chosen frame was fed into the GH-CA model directly as an initial condition. We arbitrarily let the excitatory state level (E) be 7, refractory state level (R) be 1 and the threshold value be 0.3. For the spiral wave (Fig. 6), instead of median-filtering one frame as the initial condition, all frames from the recording were filtered.

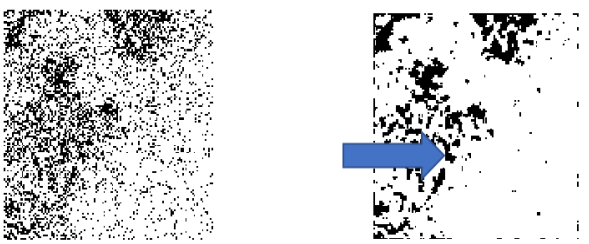

Figure 5. For the planar wave, the left image is the raw data from our experiment converted to be a matrix appearing to be noisy; the right image is the left image that has been median filtered, we can see (at the arrow) a very clear front wave compared to the left image.

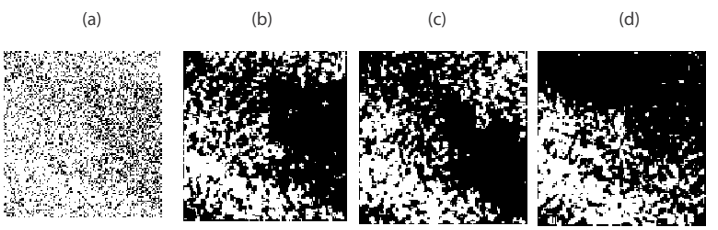

Figure 6. For a spiral wave, (a) a chosen starting frame of the raw data from our experiment converted to be a matrix appearing to be noisy; (b) is image (a) after it has been median filtered; since all frames of the raw data have been filtered, (c) and (d) represent the spiral wave at two later time points from (b), we can clearly see a wave spiraling into the center of the plate in the experiment.

Results

Following the Fraction Method, for a simple planar wave, we observed a rather constant $\frac{\#ofexcitedcells}{\#ofunexcitedcells}$ ratio after the FHN model is caught up with the GH-CA model at about the 60th GH-CA iteration (Fig. 7). A planar wave (i.e. simple wave) in the cellular automaton model is always better aligned with its FitzHugh-Nagumo model of the same initial condition than a spiral wave. We show in Fig.7 that the ratio from the FHN and CA simulations becomes the same at 0.05 as iteration step continues to 100, which indicates the two models are behaving the same with a planar wave initial condition. In contrast, when applying the Fraction Method with a spiral wave I.C.to both the FHN and GH-CA models, we saw a strong deviation between the ratio between excited and unexcited cells as iteration steps increase for both models. Since a CA wave travels faster than an FHN wave because of its state's discreteness, the CA was iterated for 100 steps and the FHN was iterated for 872 steps, which achieve the same 'cell distance'. Evidently in Fig.8, the fraction method traced the FHN simulation dynamics of a spiral wave until the wave disappears at the end of its simulation at the edges of the 2D FHN matrix, which was why its excited to unexcited cells ratio dropped dramatically to 0 at its 780 iteration step. However, it the FHN spiral wave behaviors is still captured by the fraction method precisely. In contrast, the GH-CA simulation whose IC was given by CA at a certain instant never completely left the edges of the 2D GH-CA matrix. Therefore, its excited to unexcited cells ratio was significantly higher than that of the FHN simulation around 50 GH-CA iterations. However, regardless of whether the spiral wave exits the 2D array or not, a noticeable discrepancy between the excited to unexcited cell count ratio can be seen between the GH-CA (red) and the FHN (blue) models.

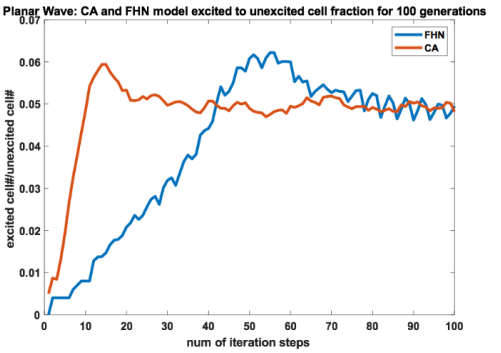

Figure 7. Fraction method performed to a simple planar wave initial condition given to the FHN (blue) and GH-CA (orange) models for 100 GH-CA and FHN iterations.

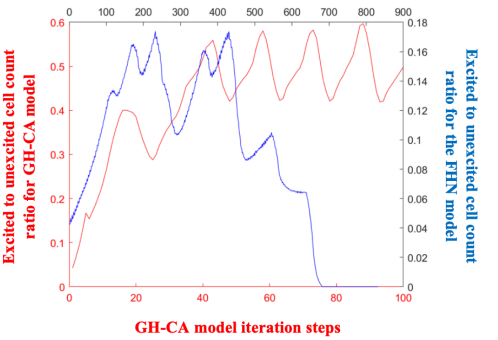

Figure 8. Fraction method performed to a complex spiral wave initial condition given to the FHN (blue, bottom line) and GH-CA (red, top line) models for 100 GH-CA iterations and 872 FHN iterations which travel the same cell equivalent distance.

We quantified the degree of overlap between the CA model simulation using the **Overlap method**. We were able to generate the degree of overlap of a planar and a spiral wave compared between the FHN and CA models. We directly compared the CA and FHN models for five different CA thresholds (color-coded) shown in Fig. 9. We can see 1) the cellular automaton model's planar waves are better aligned with the FHN models initiated by the same I.C. than the spiral waves, and 2) the fit with the spirals decreases as the number of iterations increase, while the plane waves do not decrease as much.

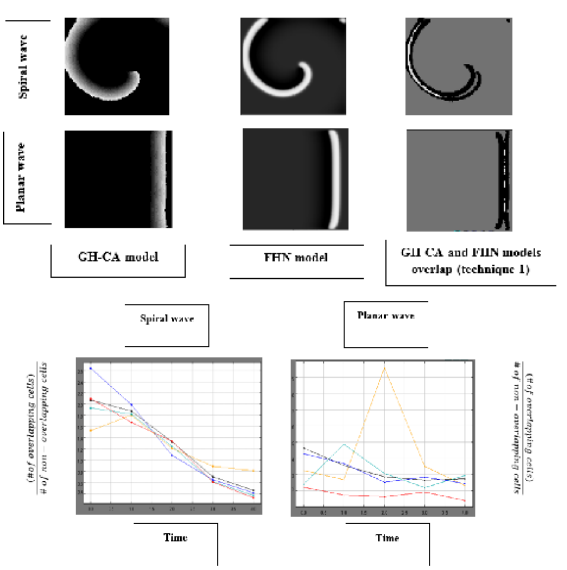

Figure 9. Overlapping to non-overlapping cells ratio between GH-CA and FHN models by capturing the maximal overlap after allowing the FHN simulation to run 200 iterations ahead of the GH-CA one and let the latter to catch up.

Furthermore, our method of initializing the CA with one frame of median-filtered real-time experimental cardiac tissue data was successful in reproducing the behavior of the raw data for the planar wave (Fig. 10), but not for the spiral wave. As for the spiral wave, its initial condition evolves to be a planar wave rather than spiraling into the center.

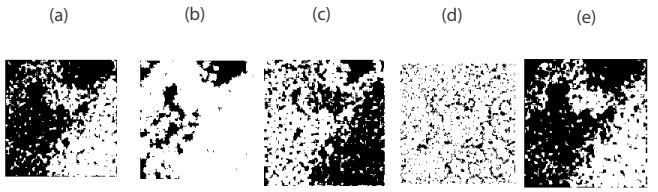

Figure 10. After a median-filtered initial condition of the experimental result of a planar wave (a) have been fed into a GH-CA model, (b) – (e) shows this planar wave's wave propagation evolution, successfully reproduced the raw data.

Discussion

Discussion of results and possible improvements

We used the FitzHugh-Nagumo model to generate data sets of simple and complex propagating waves in excitable media. We evaluated whether a cellular automaton model can reproduce these wave dynamics using two algorithmic tests, a '*fraction method*' and an '*overlap method*'. For future work, since we chose our 2D matrix cell size to be 100 for both the GH-CA and the FHN models, we could try varying the size of our simulation to see if it changes our results. For all results generated other than experimental result simulation, we relied on the condition that the GH-CA and the FHN models were initiated by the same I.C.. This was retrieved from the FHN voltage values at a certain instance and converted into discrete cell states that the GH-CA model can accept as an IC too (see Methods). We strictly used the parameter *a* from the FHN model to set the ranges for the excited and refractory cell states. In addition, we assigned a 1 for all FHN values in the "excited range" and an E+1 for all that's in the "refractory range". Both parameter assignments increase the probability that the discrete values we converted the FHN values to may not be entirely representative of the original FHN simulation, which can affect the consequent GH-CA simulation results and the comparison results between the two model.

Proposed strategies of integrating Machine Learning techniques into our GH-CA model to lessen the deviation of its simulation from experimental data

Our future strategy to resolve the challenge of spiral wave experimental data initial condition not being able to induce spirals is inspired by Gilpin's (6) recent paper "*Cellular automata as convolutional neural networks*". Gilpin (6) showed that *any* Cellular Automaton may readily be represented using a convolutional neural network (CNN) with a network-in-network architecture. They built a CNN that can learn the dynamical rules for arbitrary CA when given videos of the CA as training data. They trained ensembles of networks on randomly sampled CA and showed that CA with simpler rule tables produce trained networks with hierarchical structure and layer specialization, while more complex CA tend to produce shallower representations. This is analogous to our results. After they confirmed that arbitrary cellular automaton may be represented by convolutional perceptrons with finite layers and units, automated training of neural networks on time series of cellular automaton images was carried out. By training ensembles of convolutional neural networks on random images and random CA rulesets. More specifically, they defined a CA as an explicit mapping between an input pixel and an output pixel. For a neighborhood size of 1, there are 512 possible neighbor state groupings (i.e. a center cell has 2^9=512 neighboring state possibilities for 3-by-3-pixel groups in a binary image) for an input pixel. Therefore, their training data is an ensemble of randomly generated binary images where each image contains an equal number of black and white pixels on average. For each training input pixel, its output pixel ('label') is produced by the input pixel undergoing a randomly selected CA Conway Game of Life rule set. Subsequently, this CA map is applied to an ensemble of random binary images (the training data), in order to produce a new output binary image set (the training labels). They used a sufficient number of images and training data batches (500 images) to ensure that the training data contains at least one instance of each rule.

We may adapt this technique to train a Convolutional Neural Network (CNN) representing our CA with experimental median-filtered spiral wave data. Complex wave propagation such as a spiral wave presents dynamical rules to be learnt by the CNN like Conways' Game of Life. The input training data would be our experimental data at time with frame n, its output label data would be the experimental data at time t+1 of frame n+1. Iteratively, the next training image would be frame n+1 whose output label is frame n+2. An initial step would be to train the CNN representing our CA on synthetic wave data generated by the FHN model where its continuous values are converted into equivalent discrete states of CA values. This procedure is promising to adeptly train a CNN for leaning spiral wave propagation with an ability surpassing that of a GH-CA model.

Conclusion

We compared the dynamics of two models of cardiac propagation: a discrete Greenberg-Hastings Cellular Automaton (GH-CA) model and a continuous FitzHugh-Nagumo (FHN) model for excitable propagation. Our results were able to confirm our hypothesis that the divergence between the two models are due to initial condition (IC) complexity (i.e. the more complex the I.C. is, the faster the GH-CA simulation results deviate from the FHN model results where we treat our FHN simulation as our ground-truth surrogate experimental data). This was shown by the alignment between the CA model of a planar wave (i.e. simple) and the FHN model remaining constant, while the degree of overlap between the CA and FHN models decreasing for a spiral wave (i.e. complex) at higher time steps. Once a median-filtered frame of real-time cardiac tissue experimental data was fed to the CA model as an initial condition, the planar wave simulation propagates forward as the experimental data shows, but the spiral wave CA simulation did not successfully spiral in. This result further identifies the issue that a simpler I.C. such as a planar wave can be modelled more accurately by CA than a complex I.C. such as a spiral wave.

Acknowledgements

This project was a fulfillment for the course PHGY 461 D1/D2: Experimental Physiology at McGill University. The author would like to thank McGill M.Sc. candidate Miguel Romero Sepulvida for generously providing experimental data for simulation results of this paper and Harvard NSF-Simons Research Fellow Dr. William Gilpin for fruitful discussions and further collaboration on Convolutional Neural Network as Cellular Automata model for our cardiac experimental data. Especially, the author would like to sincerely thank her supervisor Dr. Gil Bub from McGill's Department of Physiology for continuously offering his patience, intellectual guidance, stimulating discussions and support.

References

1. Bub G, Shrier A, Glass L. Global organization of dynamics in oscillatory heterogeneous excitable media [Internet]. Physical review letters. U.S. National Library of Medicine; 2005 [cited 2020Jan15]. Available from: https://www.ncbi.nlm.nih.gov/pubmed/15698236

2. Bub G. Contents [Internet]. Optical Mapping of Pacemaker Interactions. [cited 2020Mar7]. Available from: https://www.physiol.ox.ac.uk/~gb1/cnd/bub/thesis.html#tth_sEc1.3

3. Burton RAB, Klimas A, Ambrosi CM, Tomek J, Corbett A, Entche-

va E, et al. Optical control of excitation waves in cardiac tissue [Internet]. Nature photonics. U.S. National Library of Medicine; 2015 [cited 2020Jan15]. Available from: https://www.ncbi.nlm.nih.gov/pmc/articles/PMC4821438/

4. Ccoffinn: Automated Wave Tracking in Cultured Cardiac ... [Internet]. [cited 2020Jan15]. Available from: https://www.cell.com/biophysj/pdf/S0006-3495(16)30816-5.pdf

5. FitzHugh R. Impulses and Physiological States in Theoretical Models of Nerve Membrane [Internet]. Biophysical Journal. Cell Press; 2009 [cited 2020Jan15]. Available from: https://www.sciencedirect.com/science/article/pii/S0006349561869026

6. Gilpin, William. Cellular automata as convolutional neural networks [Internet]. arXiv.org. 2019 [cited 2020Jan15]. Available from: https://arxiv.org/abs/1809.02942

7. Murray JD. Mathematical Biology - I. An Introduction: James D. Murray [Internet]. Springer. Springer-Verlag New York; [cited 2020Jan15]. Available from: https://www.springer.com/gp/book/9780387952239

8. Pálsson E, Cox EC. Origin and evolution of circular waves and spirals in Dictyostelium discoideum territories [Internet]. Proceedings of the National Academy of Sciences of the United States of America. U.S. National Library of Medicine; 1996 [cited 2020Mar7]. Available from: https://www.ncbi.nlm.nih.gov/pmc/articles/PMC40047/